Materials Science-Poland, 42(2), 2024, pp. 52-69
http://www.materialsscience.pwr.wroc.pl/
DOI: 10.2478/msp-2024-0021

Retrofitting of heat-damaged fiber-reinforced concrete cylinders using welded wire mesh configurations

Aref A. Abadel*

Department of Civil Engineering, College of Engineering, King Saud University, Riyadh 11421, Saudi Arabia

Fire damage poses a significant risk to reinforced concrete structures throughout their lifespan. Fire exposure influences the stress-strain properties and durability of concrete, despite its non-flammability. Therefore, the strengthening approach is an economic option for lengthening their lifespan. This paper aims to conduct an experimental investigation into retrofitting heat-damaged fiber-reinforced concrete cylinders using welded wire mesh (WWM) configurations. Four concrete mixes were investigated. In total, 48 concrete cylinders were tested under axial compression until failure. The primary variables considered in the testing program consisted of (i) the influence of various fiber types (steel fiber (SF), polypropylene (PP), and hybrid fibers (SF+PP)); (ii) exposure temperature (26°C and 600°C); and (iii) WWM strengthening. Exposure to a temperature of 600°C led to a significant reduction in the compressive strength, ranging from 23.7% to 53.3%, while the inclusion of fibers has a substantial effect on the compressive strength of concrete, regardless of fiber type, with an increased ratio reaching up to 34.7%. The finding also clearly shows that the strengthening of heat-damaged specimens with WWM jacketing resulted in a 38.8%, 4.9%, and 9.4% increase in compressive strength for SF, PP, and SF+PPF specimens, respectively, compared to unheated control specimens. The suggested approaches to strengthening, which involve the use of WWM jacketing with two layers, successfully restored and surpassed the initial concrete compressive strength of the specimens that were damaged due to exposure to high temperatures.

Keywords: *compression strength, elevated temperature, fiber-reinforced concrete, retrofitting, stiffness, WWM jacketing*

1. Introduction

Concrete structures can experience substantial degradation when subjected to elevated temperatures, such as those encountered in fires. A study has been carried out to investigate the impact of high temperatures on concrete structures and strategies to reduce this deterioration. Research has examined the remaining strength of concrete cylinders following exposure to fire at various temperatures [1]. A literature review on the influence of temperature on concrete strength uncovers various significant discoveries. The research conducted by Shaikh and Vimonsatit [2] provides evidence that when concrete is exposed to high temperatures, its compressive strength decreases, independent of the methods used for cooling. Abadel et al. [3] studied the influence of plain and fiber-reinforced concrete (FRC) under different temperature and cooling regime environments. The results demonstrated that FRC shows better residual strength compared to concrete without fiber. Li et al. [4] discovered that the compressive strength of concrete falls significantly when subjected to temperatures ranging from 400°C to 600°C. The greatest reduction in strength was observed at temperatures between 600°C and 800°C. Moreover, studies have investigated the assessment of both the static and dynamic mechanical characteristics of heat-damaged concrete, specifically in constructions such as auxiliary buildings for nuclear reactors [5]. Research has also concentrated on the restoration of pre-damaged concrete through techniques such as post-tensioned steel straps [6]. A study conducted by Abadel and Alharbi [7] examined the efficacy of several strengthening methods, such as FRP confinement and steel strapping, in improving the performance of pre-damaged concrete cylinders. Typically, concrete constructions possess a comparatively elevated level of fire resistance, enabling them to endure fire exposure without significant damage. Therefore, it is important to explore

* E-mail: aabadel@ksu.edu.sa

methods for repairing the damaged sections or restoring the structural capacity following a fire. This can lead to significant economic benefits by avoiding the expenses associated with demolition and reconstruction. To determine the expenses associated with repairing the structure, it is important to evaluate the extent of the fire-induced damage. Several investigations have been carried out on diverse characteristics of concrete subjected to fire or high-temperature conditions (e.g. References [3, 8–21]). Furthermore, the resilience of concrete structures following exposure to elevated temperatures has been a topic of investigation. Research suggests that ordinary strength concrete typically remains usable after fire incidents, although its long-term durability may be compromised [22, 23]. Methods such as impact-echo testing and computational modeling have been used to evaluate damage in concrete cylinders and provide techniques for identifying damage [24, 25]. Li et al. [26] examined the static and dynamic mechanical characteristics of concrete both before and after being subjected to high temperatures. The compressive strength had a significant loss at a critical temperature of 400°C. As the temperature continued to rise from 400°C to 800°C, the decrease in strength became increasingly pronounced.

Chen et al. [27] examined the synergistic impact of increasing strain rate and temperature on normal-strength concrete (NSC) at temperatures ranging from 20°C to 950°C. The findings indicate that as the temperature rises to 400°C, there is a higher occurrence of cracks and they propagate at a significantly faster rate compared to what is found at room temperature. Moreover, as the temperature rose from 400°C to 950°C, the cracks exhibited reduced severity and propagated at a slower rate with the escalating temperature. Concrete exhibits significant strain rate effects on its stress-strain curve even when subjected to high temperatures.

Xiao et al. [28] investigated the impact of strain rate on the compressive response of high-strength concrete (HSC) following exposure to extreme temperatures ranging from 20°C to 800°C. The test results demonstrate a negative correlation between elevated temperatures and both elastic modulus and residual compressive strength. Conversely, an increase in strain rate is positively associated with an increase in both elastic modulus and residual compressive strength.

In their study, Poon et al. [29] examined the strength and durability of pozzolanic concretes that contained blast furnace slag, silica fume, and fly ash. These concretes were subjected to high temperatures of up to 800°C. Pozzolanic concretes with blast furnace slag and fly ash exhibit superior performance, especially at temperatures below 600°C, as compared to concretes made solely with pure cement. The high-strength pozzolanic concretes exhibited a significant decrease in durability linked to permeability, compared to the decrease in compressive strength. Additionally, it was discovered that substituting 30% of cement with fly ash in HSC and replacing 40% of cement with blast furnace slag in NSC is the most effective way to maintain the highest levels of strength and durability following exposure to high temperatures.

Bastami et al. [30] examined the effects of elevated temperatures on HSC cylinders that were heated to 800°C. Their study specifically investigated the influence of water/cement and aggregate-to-cement ratios. The results indicated that both ratios had a substantial impact on compressive strength. Specifically, larger water/cement ratios resulted in increased strength after being exposed to high temperatures.

Extensive studies have thoroughly examined the impact of elevated temperatures on the strength and stiffness of concrete. Spalling, which is caused by the presence of trapped water vapor, has been seen as a result. To tackle this issue, a novel method utilizes polypropylene (PP) fibers that undergo melting when exposed to high temperatures. This melting process facilitates water drainage and enhances the material's porosity, specifically at a temperature of 170°C [31]. Scientists have investigated the combination of steel fibers with different materials to enhance their ability to withstand high temperatures [32]. Furthermore, research has demonstrated that the use of polypropylene fibers in self-compacting concrete can effectively inhibit spalling. Moreover, a combination of steel and polypropylene fibers has been found to improve both fire resistance and mechanical qualities [3].

Bayasi and Al Dhaheri [33] examined the performance of PP FRC when subjected to high-temperature conditions. The study showed that the maximum bending strength of PP FRC diminishes as the exposure temperature and duration increase. Furthermore, the flexural behavior of PP FRC is mostly unaffected by exposure to temperatures below 100°C. Xiao and Falkner [24] performed an empirical investigation on the enduring capacity of high-performance concrete (HPC) with and without PP fibers under various increased temperatures. The study showed that incorporating PP fibers into HPC does not adversely impact the residual compressive and flexural strengths following exposure to elevated temperatures.

In their study, Bangi and Horiguchi [34] examined how the shape and kind of fibers impact the maximum pore pressures in high-temperature conditions of fiber-reinforced high-strength concrete (HSC). Measurements of pore pressure indicated that the inclusion of organic fibers, independent of their kind, had a substantial impact on reducing pore pressure in heated high-strength concrete (HSC). PP fibers exhibited superior effectiveness in reducing the development of maximum pore pressure in comparison to polyvinyl alcohol fibers, but steel fibers had a somewhat lesser impact.

Novák and Kohoutková [35] examined the fire behavior of FRC under high temperatures. The findings indicated that the tensile and compressive strength of FRC exhibited a decline as the temperature increased. At temperatures of 400°C and 600°C, the remaining compressive strength is approximately 60% and 35% of the original value, respectively. The decrease in strength is mostly attributed to the structural degradation of the specimen resulting from the heightened porosity and formation of cracks.

Varona et al. [36] reported the test findings of six combinations of FRC with varying strengths, using limestone aggregates. These mixtures were subjected to increased temperatures before being tested. The obtained results were consistent with prior research, and formulas were developed to evaluate the remaining compressive and flexural strengths following exposure to high temperatures. The flexural strength tests also assessed ductility, and the findings indicated that the utilization of steel fibers with a greater aspect ratio could result in reduced ductility following exposure to temperatures over 650°C.

Concrete cylinders can be strengthened using different techniques that utilize materials such as welded wire mesh (WWM) and ferrocement. Welded wire mesh and geotextile materials are recognized for their economical nature, exceptional strength-to-weight ratio, and ability to work well with concrete, making them appropriate for strengthening concrete buildings [37]. In addition, the utilization of welded wire mesh for axial reinforcement has been demonstrated to improve the ability of concrete elements to bear loads [10]. The application of ferrocement to strengthen concrete cylinders has been investigated, with research specifically examining the use of nickel-titanium SMA wires for prestressing [38].

Research has been carried out in the field of ferrocement to investigate the reinforcement of concrete columns using ferrocement jackets. The findings have demonstrated promising outcomes in improving the load-bearing capacity of the columns [39–42]. Furthermore, a study conducted by Alobaidy et al. [43] has examined the shear performance of ferrocement beams that are reinforced with steel wire mesh. The findings suggest that these beams exhibit enhanced crack loads, service loads, ultimate loads, and toughness when compared to alternative reinforcement materials. Ferrocement has been suggested as a technique to reinforce short concrete columns subjected to axial loading, demonstrating its ability to improve the structural behavior of concrete elements [44].

Ferrocement has been recognized as a highly promising material for enhancing the strength of concrete constructions, particularly cylinders. Studies have demonstrated that the utilization of ferrocement jackets is an effective method for repairing and reinforcing reinforced concrete columns, resulting in enhanced structural performance [40]. In addition, research has shown that the application of reactive powder concrete jackets and fiber-reinforced polymer wrapping can

improve the axial and flexural performance of circular reinforced concrete columns, demonstrating the efficacy of these strengthening methods [45].

Furthermore, research on the utilization of ferrocement composites to reinforce concrete columns has emphasized the benefits of this material in improving the ability to withstand heavy loads and maintaining the structural soundness of concrete components [46]. Research has also investigated the effect of using ferrocement confinement on the behavior of concrete, with a focus on its beneficial impact on the mechanical qualities of concrete structures [47].

To summarize, the existing literature on strengthening concrete cylinders using ferrocement highlights the material's adaptability and efficacy in improving the structural integrity of concrete components. Currently, there is a scarcity of studies investigating the enhancement of heat-damaged fiber concrete components through the utilization of welded wire mesh jacketing. The main aim of this experimental investigation is to evaluate the efficiency of using welded wire mesh jackets as a strengthening scheme for heat-damaged fiber concrete cylinders.

2. Experimental Program

2.1. Materials

This study used a normal-strength mix with coarse aggregate sizes of 20 and 10 mm, aiming for a cylinder compressive strength of 30 MPa after 28 days. The materials that were utilized in the production of all concrete cylinders consisted of ordinary Portland cement (Type I) possessing a specific gravity of 3.15; natural silica sand with a fineness modulus of 1.65 and a specific gravity of 2.60, while the specific gravities for the coarse aggregates and crushed sand were 2.781% and 2.567%, respectively; tap water; and a superplasticizer (melamine formaldehyde sulfonated) with a specific gravity of 1.21. To ensure consistent workability, the superplasticizer was used in all mixtures. Fiber-reinforced concrete was prepared using hooked-end steel (SF) and polypropylene fibers (PP), which were purchased from local market suppliers. The tensile strengths of SF and PP were 1225 and 550 MPa, respectively, while their elastic modulus was 200 and 4 GPa, respectively. The rectangular PP fibers had dimensions of 0.6 mm in thickness, 1 mm in width, and 50 mm in length. The diameter and length of the circular SF were 0.75 mm and 60 mm, respectively. The SF and PP fibers had specific gravities of 7.85 and 0.9, respectively. Figure 1 and Table 1 show the characteristics of the fibers used in the study.

Table 1. Physical and mechanical properties of fibers

Properties	**Fiber Type**	
	Polypropylene (PP)	**Steel (SF)**
Shape	Crimped	Hooked ends
Length (mm)	50	60
Section dimensions (mm)	1.0 × 0.6 (Rectangular)	0.75 (Circular)
Specific gravity	0.90	7.85
Modulus of elasticity (GPa)	4.0	200
Tensile strength (MPa)	550	1225

2.2. Mix proportions

Table 2 shows the component quantities used to prepare normal-strength concrete mixes. Table 3 presents the distribution of SF, PP, or hybrid fibers in terms of volume (or by weight) within the concrete mixes. It is important to mention that in Table 3, the abbreviations "M-C0", "M-SF", "M-PPF", and "M-SF+PPF" are used to denote several types of mixes, namely: mixes without SF and PP, mixes with SF fibers only, and mixes with a combination of SF and PP fibers, respectively. Table 3 displays the test matrix used in this study's experimental program. All test cylinders were replicated three times for the unheated, heated, unstrengthened, and strengthened specimens to ensure the consistency of the data and enhance confidence in the findings of this study. The specimens in this

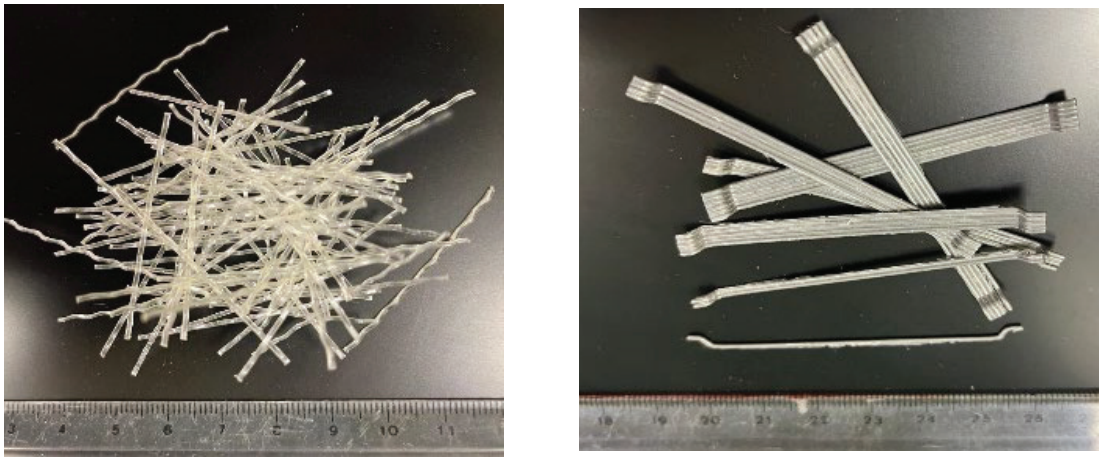

(a) (b)

Fig. 1. The fibers utilized in this study: (a) crimped polypropylene and (b) Hooked-steel.

Table 2. Mix proportions used for concrete in kg/m^3

Material	Weight
Cement	378
Crush sand	294
Silica sand	489
Coarse aggregate ($d_{agg.}$= 20 mm)	675
Coarse aggregate ($d_{agg.}$ = 10 mm)	320
Water	190.5
Super-plasticizer	1.0 Liters

investigation were 48 concrete cylinders that had a diameter of 150 mm and a height of 300 mm. The primary variables considered in the testing program consisted of (i) the influence of various fiber types (SF, PP, and hybrid fibers), (ii) exposure temperature (26°C and 600°C), and (iii) WWM strengthening.

2.3. Specimen preparation

The cylinder specimens were fabricated by molding. To prepare fiber-reinforced concrete, cement, sand, and gravel were first mixed in the desired mixtures. Water was added to the dry mix, and then stirred to make a uniform concrete slurry. The distribution of the fibers in the concrete mixture is a vital factor that significantly influences the mechanical properties of concrete. Therefore, the fibers were then added gradually to the mixer while mixing continued to ensure that the fibers were evenly distributed without forming clumps. The mixing continued for an additional 5 minutes to achieve a uniform distribution of the fibers. To mitigate segregation, the concrete mix was gradually poured into the designated molds. Additionally, a vibrator was used to carefully shake the concrete, preventing the formation of voids. Figure 2 shows the cylinder specimens on the vibration table during their pouring into the molds. The upper surface was carefully leveled using a steel trowel to guarantee a flat surface, and the stresses were not concentrated during the test. We submerged the specimens in a water tank for 28 days to undergo a curing process.

2.4. WWM strengthening

Table 4 presents the features of the WWM used in the specimen strengthening. The WWM had a hole size of 13 mm and a diameter of 0.6 mm. Table 4 also presents the properties of the mortar employed in the WWM jacketing. The sandblasting procedure was applied to the concrete surface to create a roughened surface, hence improving the adhesive strength between the strengthening materials and the concrete surface, as shown in Figure 3(a). Prior to the application

Table 3. Test matrix

Concrete mix	Specimens ID	Percentage of fiber by volume			Temperatures	Strengthening	No. of specimens
		Polypropylene (PP)	Steel (SF)	Total			
M-C0	C0-RT	–	–	–	26°C	–	3
	C0-600				600°C		3
	C0-RT-S				26°C	WWM	3
	C0-600-S				600°C		3
M-SF	SF-RT	–	0.6	0.6	26°C	–	3
	SF-600				600°C		3
	SF-RT-S				26°C	WWM	3
	SF-600-S				600°C		3
M-PPF	PPF-RT	0.2	0	0.2	26°C	–	3
	PPF-600				600°C		3
	PPF-RT-S				26°C	WWM	3
	PPF-600-S				600°C		3
M-SF+PPF	SF+PPF-RT	0.2	0.6	0.8	26°C	–	3
	SF+PPF-600				600°C		3
	SF+PPF-RT-S				26°C	WWM	3
	SF+PPF-600-S				600°C		3
		Total No. of specimens					48

Fig. 2. Concrete cylinders during casting

Table 4. WWM and mortar properties

	Material	Unit	Values
WWM	Thickness per layer	mm	0.6
	Elastic modulus	MPa	108
	Yield stress	MPa	382
	Ultimate stress	MPa	544
Mortar for WWM composite	Compressive strength-28 day	MPa	45
	Tensile strength-28 day	MPa	3.8
	Bond strength	MPa	0.79

of the WWM strengthening, the concrete surface underwent cleaning to eliminate any waste particles from the sandblasting procedure. Prior to applying the WWM jacketing, a 2 mm coating of adhesive mortar was placed on the concrete surface. The first layer of WWM was implemented and carefully pushed into the mortar layer, as shown in Figure 3(b). An additional application of adhesive mortar was carried out to cover the WWM completely, as shown in Figure 3(c). The second layer of WWM was applied using the same processes as the first layer. A 10 mm gap was kept at the ends of the specimens to prevent the direct application of load to the WWM during testing. Figure 3(d) shows the final appearance of the specimens after being strengthened with WWM jackets.

2.5. Heating of specimens

Prior to heating, the specimens were allowed to dry naturally for 120 days following the end of the 28-day curing phase. This procedure is used to guarantee that the specimens are completely dry and to manage any potential shrinkage strain or explosion brought on by the abrupt temperature increase. As shown in Figure 4, the specimens were heated using an electrical oven with internal dimensions of 1.0 × 1.0 × 1.0 m. The cylinders were

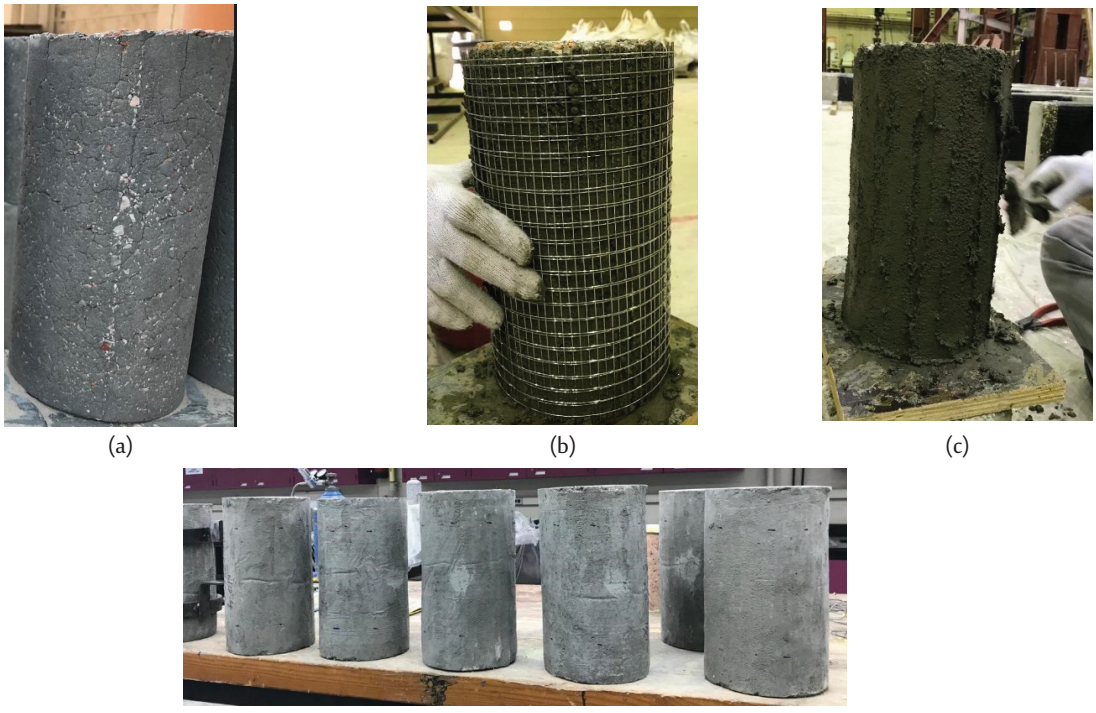

Fig. 3. Heated cylinders after (a) sandblasting procedure, (b) WWM jacketing, (c) mortar layer, and (d) final appearance

subjected to a controlled heating process, increasing their temperature from the ambient temperature (i.e., 26°C) to the predetermined target temperature (i.e., 600°C) at an average rate of 8°C per minute. Figure 5 displays the time-temperature curve used for heating the cylinders. Figure 5 illustrates the typical temperature-time curve employed for conducting structure fire resistance tests according to ISO 834 [49]. The figure clearly demonstrates that the oven utilized in the current investigation was incapable of attaining fast heating rates that simulate those of a typical fire. Nevertheless, it is important to note that the typical fire test may not accurately simulate the true heating of concrete in an actual building during a genuine fire [3]. The factory-supplied Type-K thermocouples were used to measure the internal temperature of the oven. The cylinders were exposed to a high temperature of 600°C for a duration of 3 hours to guarantee that the temperature was evenly distributed inside the cylinder. Following the heating cycle, the cylinders were left to cool before testing and strengthening.

Fig. 4. Specimens inside the electrical oven prepared for heating

2.6. Testing procedure

The cylinders tested in this study were subjected to an axial compression load to determine the stress-strain relationship. The cylinders were topped with sulfur on their top surface to ensure a perfectly flat surface for conducting the test. An

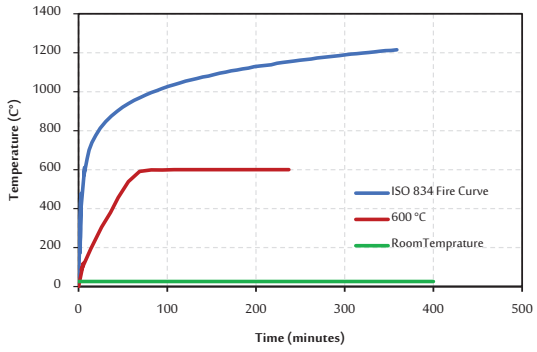

Fig. 5. The time-temperature curves employed in this research

Fig. 6. Test setup used in this research

axial strain measurement was conducted using a compressometer equipped with two Linear Variable Differential Transformer (LVDTs) positioned around the specimen, as illustrated in Figure 6. The cylinders were subjected to compressive pressure at a rate of 0.2 MPa/s until failure, following the procedure suggested by ASTM C39 [50].

3. Results and Discussion

3.1. Failure patterns

Figure 7 shows typical examples of failure modes observed in control and strengthened specimens following compression tests and exposure to heating. The control samples (without fibers) had brittle failure due to concrete crushing, as shown in Figure 7. The control samples (without fibers) subjected to high temperatures exhibited a reduced tendency for brittle failure. At first, the concrete showed premature cover spalling. Subsequently, there was a failure when the axial load was decreased in comparison with samples of the same kind that were subjected to room temperature. The concrete exhibited a modest apparent visual discoloration under exposure to a temperature of 600°C. Thermal cracking was noted on the concrete's surface of specimens without fibers at 600°C. However, the failure mode of the heated specimens was remarkably similar to that of the unheated specimens. There are fewer instances of violent failures when compared to the unheated specimens. The C0-RT specimens exhibited significant cracks and crushing of the concrete, first in the upper portion (i.e., the loading point), and then at the middle points of the specimen. Initially, the concrete cover exhibited premature spalling, which was subsequently followed by failure at its strength capability. The same trend was noticed in the PPF-RT, where the cracks started from the loading point to the middle points of the specimen, in comparison with the SF-RT and SF+PPF-RT specimens. Nevertheless, the presence of fibers in mixes prevented thermal cracks on the surface. The crack widths of the specimens with steel fibers (i.e., SF-RT and SF+PPF-RT) were smaller than those of the specimens without fibers (i.e., C0-RT and PPF-RT). In addition, the C0-RT and PPF-RT specimens exhibited narrower cracks compared to the SF-RT and SF+PPF-RT specimens. This result may be attributed to the incorporation of SF, PP, and SF+PP fibers in concrete specimens creating a bridging influence between cracks, similar to the outcomes mentioned in previous studies (e.g., [51, 52]). The inclusion of fiber can change the failure mode from brittle to ductile by enhancing the concrete's toughness, aligning with findings from previous studies [53, 54]. In general, the specimens without fibers failed in explosive/brittle mode. Conversely, this did not occur in the specimens that had fibers (i.e., became less explosive/brittle) due to the random distribution of the fibers within the concrete matrix. When specimens containing PP

fibers were preheated to temperatures of 600°C, the failure of the specimens became more ductile. This can be attributed to the fibers melting, leading to the development of pores within the concrete core. In addition, when SF specimens were subjected to temperatures of 600°C, the failure exhibited increased ductility compared to the specimens without fibers. However, it still displayed greater brittleness than the specimens containing PP fibers. The failure mode of heated specimens containing hybrid fibers exhibited characteristics that fell between those of specimens containing only SF and those containing only PP fibers. Figure 7 is a typical photograph of the failure mode of all the cylinders strengthened with WWM jackets in comparison to the control specimens. Generally, as loading increased, small cracks on the mortar surface that enveloped the WWM were observed. The cracks progressively expanded and grew wider until reaching their peak strength. At this point, the cracks reached their maximum length at the ends of the cylinders' cross-sections, coinciding with a rapid decrease in the resisting load. The WWM failed across the specimen's height, which led to the failure of the specimens. Close to the maximum load, the WWM layers were seen to expand outward before experiencing a rapid failure. In some of the specimens, vertical cracks were observed across the specimen's height, as shown in Figure 7. The cylinders strengthened with WWM jackets experienced failure on the ends (i.e., loading point), followed by further failure at the midpoint. The strengthened specimens subjected to higher temperatures showed reduced susceptibility to brittle failure in comparison to the specimens subjected to room temperature (26°C). In general, the heated specimens produced a quieter sound, while the unheated specimens failed suddenly with a loud explosive sound. The observed test behavior and failure manner indicated that the transverse wires in unheated specimens (i.e., C0-RT-S, SF-RT-S, PPF-RT-S, and SF+PPF-RT-S) experienced hoop tension, resulting in the generation of passive confinement pressure. As the load increased, more prominent and broader cracks became visible, eventually resulting in the separation and protrusion of the mortar, especially in the C0-600-S, SF-600-S, and PPF-600-S specimens, as shown in Figure 7. Several meshes obtained from the failed specimens exhibited fractured horizontal wires, indicating that these wires yielded as a result of hoop tension.

3.2. Effect of heating exposure on compressive strength

The loss in compressive strength exhibited variability across different mixes based upon the specific type of fibers employed, as displayed in Figure 8. The investigation demonstrated that the residual compressive strength of all the concretes, regardless of the presence of fibers, declined as the exposure temperature rose. This phenomenon can be attributed to the decrease in moisture content and the breaking down of the hydrated cement paste [48]. The findings indicate that the inclusion of steel fibers alone resulted in a 34.7% increase in compressive strength at room temperature. Nevertheless, the addition of PP fibers alone led to a slight increase of 8.8% in compressive strength at room temperature. The incorporation of hybrid fibers (SF and PP) resulted in a significant enhancement in compressive strength at normal room temperature conditions. Specifically, the compressive strength increased by approximately 34.0%. The notable enhancement in compressive strength observed in the concrete with steel fibers can be attributed to the utilization of steel fibers with a larger aspect ratio of (L/d = 80) in this study, which effectively harnesses the strength of the fibers. The observed range of enhancement in compressive strength aligns with previous research findings [3, 35, 36].

After exposing the specimens to a temperature of 600°C, the degree of decrease in compressive strength ranged from 23.7% to 53.3%. The percentage loss in strength for plain concrete was 53.3%, whereas the samples with SF alone, PP alone, and hybrid of steel and PP showed a reduction of 29.9%, 45.1%, and 23.7%, respectively. The range of reduction in strength is within the range of the previous studies [15]. This clearly shows that the presence of PP fiber can contribute to enhancing the overall performance of concrete under

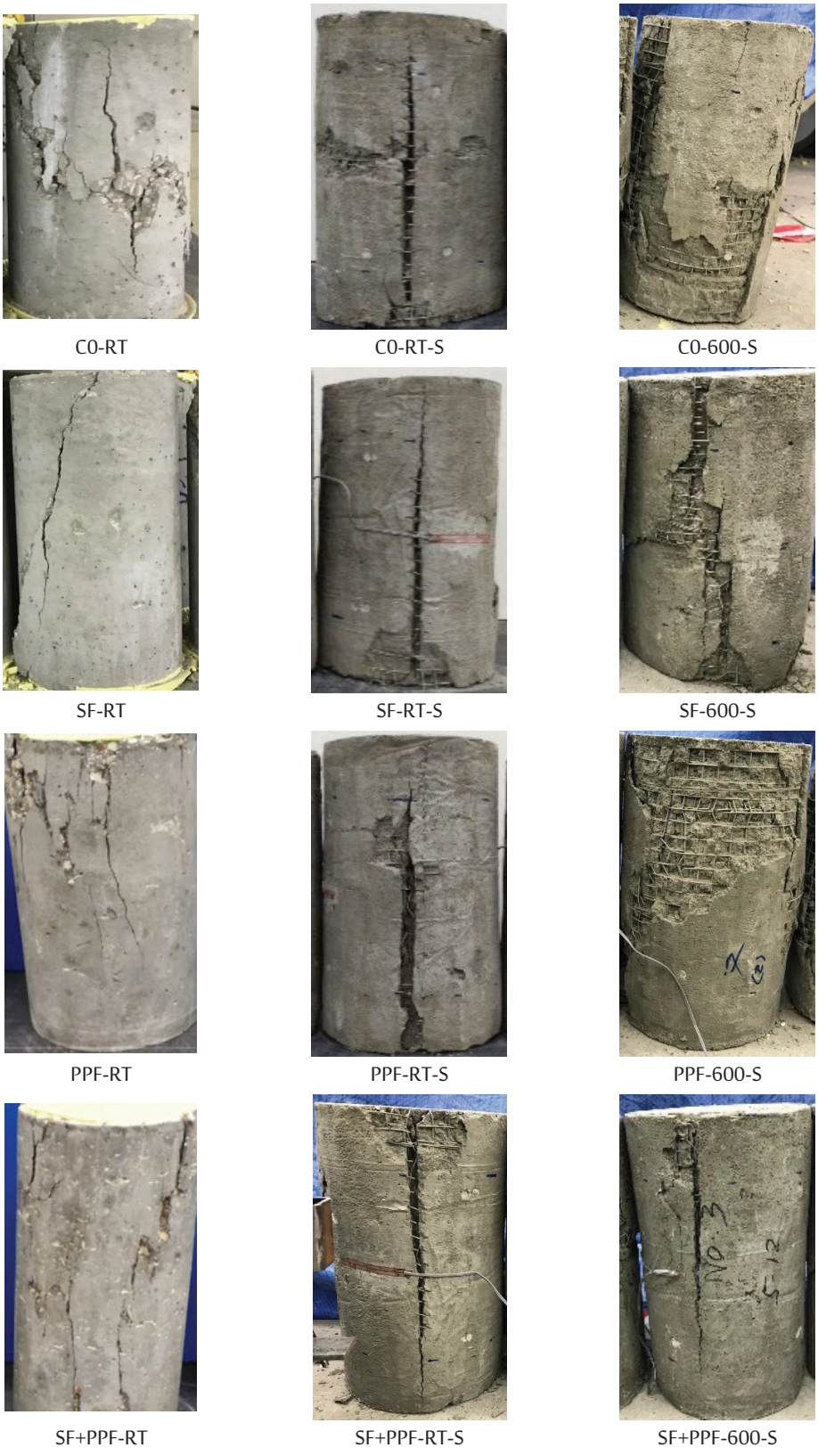

Fig. 7. Representative typical failure mode for control and strengthened specimens

high-temperature conditions due to an increase in pore volume after the melting of the fibers, potentially allowing gases to escape and thereby contributing to enhancing the compressive strength of the material [1, 7, 55].

3.3. Effectiveness of WWM strengthening

Figure 8 presents the average compressive strength of all the specimens. Based on the results, it is evident that the strengthened concrete specimens exhibited greater compressive strength in comparison to the unstrengthened specimens. This can be attributed to increased confinement due to the presence of WWM jacketing. When exposed to room temperature and enclosed in WWM jacketing, the C0-RT-S, SF-RT-S, PPF-RT-S, and SF+PPF-RT-S specimens showed an increase in compressive strength of 68.5%, 74.4%, 82.7%, and 63.2%, in comparison to the C0-RT, SF-RT, PPF-RT, and SF+PPF-RT control specimens that were exposed to room temperature, respectively. Furthermore, when exposed to a temperature of 600°C, the compressive strength of the C0-600-S, SF-600-S, PPF-600-S, and SF+PPF-600-S specimens increased by 112.1%, 98.2%, 91.7%, and 43.4% in comparison to the C0-600, SF-600, PPF-600, and SF+PPF-600 control specimens that were exposed to room temperature, respectively. Application of WWM jacketing to strengthen specimens that had been damaged by being subjected to high temperatures resulted in a 38.8%, 4.9%, and 9.4% increase in compressive strength for SF-600-S, PPF-600-S, and SF+PPF-600-S specimens, respectively, in comparison to the initial compressive strength of the undamaged specimens C0-RT, SF-RT, PPF-RT, and SF+PPF-RT. However, the C0-600-S specimen showed a slight decrease of 1% compared with C0-RT, as shown in Figure 8.

3.4. Stress-strain curves

The stress-strain response for concrete is a significant property for evaluating the overall behavior of RC structures under high temperatures (i.e., 600°C). Figures 9(a) and 9(b) show the stress-axial strain curves for unheated and heated specimens, respectively. To determine the average stress, the compressive load was divided by the cylinder's cross-sectional area. The axial strains were calculated as the ratio of the average axial displacement (as measured by the LVDTs) and the length of the gage. The elastic modulus decreases as the temperature rises from ambient (i.e., 26°C) to 600°C, which can be clearly noted in the stress-strain curves. As shown in Figure 9(a), the stress-strain curves for the unheated specimens demonstrated a generally linear trend until it reached peak strengths of 30.2, 40.7, 32.9, 40.5, 50.6, 71.0, 60.1, and 66.1 MPa for C0-RT, SF-RT, PPF-RT, SF+PPF-RT, C0-RT-S, SF-RT-S, PPF-RT-S, and SF+PPF-RT-S, respectively. The stress-strain curves demonstrated a decrease in slope, leading to a nonlinear behavior. After reaching maximum strength, the concrete had cracks that progressively widened, leading to complete failure due to the concrete splitting. The same trend was noticed in the heated specimens; the stress-strain curves for the unheated specimens demonstrated a generally linear trend until they reached peak strengths, as shown in Figure 9(b). The specimens with fibers (SF and a combination of SF+PPF) showed a gradual decline in the curve due to the ability of the fibers to bridge the cracks, which resulted in enhanced post-peak ductility, as shown in Figure 9. Although the heated specimens exhibited a decrease in compressive strength, the stress-strain curves did not have a sudden drop but rather were nearly flat curves, as shown in Figure 9(b). Analysis of those curves indicates that when subjected to a temperature of 600°C, concrete with and without fibers experiences a greater reduction in stiffness compared to a reduction in compressive strength, which will be discussed in the following section. The decrease in strength due to temperature increases can be attributed to the hydrated cement paste disintegrating and losing moisture content. Other researchers [3] have also reported similar findings, showing that the residual strength of a concrete mix with fibers significantly decreases when subjected to temperatures over 600°C. Furthermore, it is seen that the concrete with SF exhibited a superior capacity for energy absorption (the area under the stress-strain curve) and elastic modulus following exposure to high temperatures

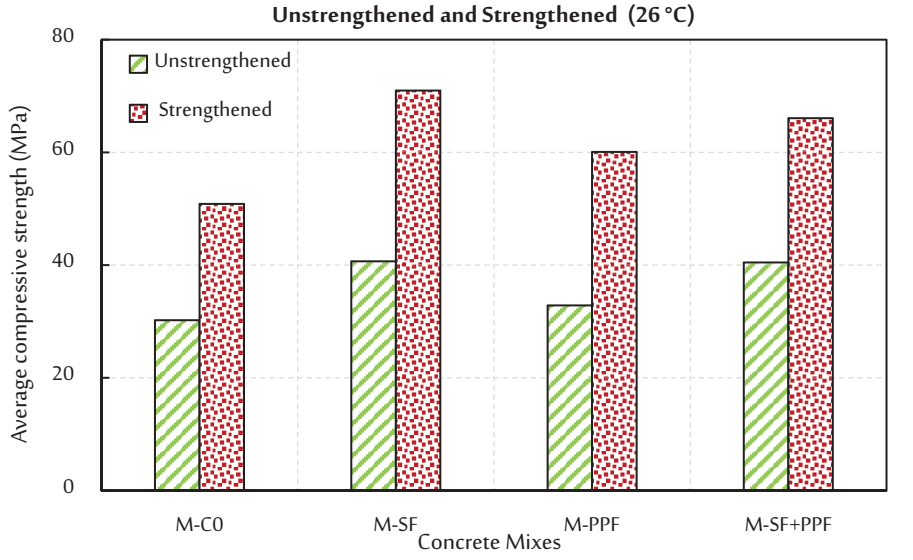

(a)

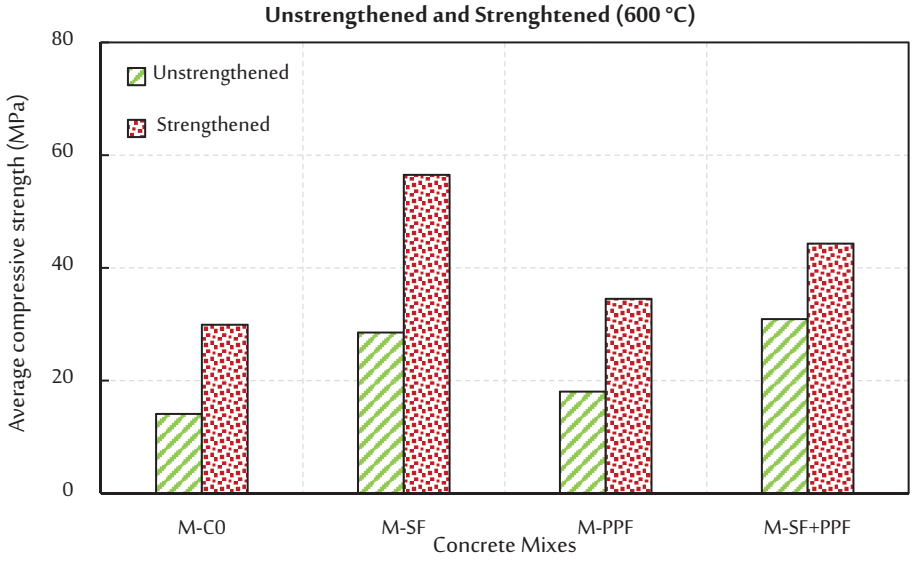

(b)

Fig. 8. Effectiveness of WWM strengthening for unheated and heated specimens: (a) room temperature and (b) heated at 600°C

in comparison to the concretes with no fibers, PP, and hybrid fibers. The reason for this is that SFs possess superior mechanical characteristics (i.e., elastic modulus and strength) compared to PP fibers, and SFs are also capable of withstanding higher temperatures. PP fibers, however, could melt when exposed to high temperatures. Furthermore, the decrease in modulus of elasticity and energy absorption capacity caused by heating was comparatively smaller in concretes that contained hybrid fibers, in contrast to concretes that just had PP fibers. The addition of SF addressed the deficiencies of the PP fibers, namely in terms of tensile strength and elastic modulus. However, the PP fibers contributed to the reduction of porosity in the concrete mix [3]. Figure 9 presents comparisons

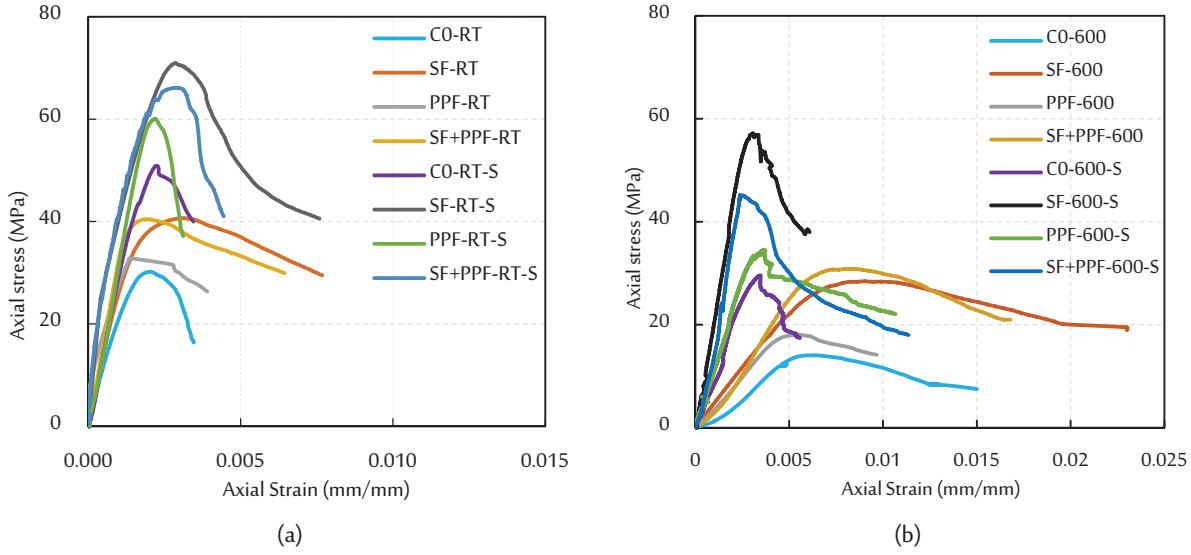

Fig. 9. Stress-strain curves for unheated and heated specimens: (a) room temperature and (b) heated at 600°C

of the stress-strain curves for the strengthened and unstrengthened specimens. The figure demonstrates that the use of WWM jacketing greatly enhanced the specimen's strength, strain at ultimate strength, and the post-peak response of all concrete mixes, regardless of whether heated or unheated. SF concrete specimens and hybrid fiber concrete specimens (i.e., SF+PPF) have shown superior performance compared to the other types of mixes (C0 and PPF specimens) in both unstrengthened and strengthened conditions. The failure of the strengthened specimens was primarily attributed to vertical crack widening caused by the yielding of the WWM with an inability to maintain the specimen's strength. The observed specimen behavior and failure pattern indicate that the WWM experienced hoop tension, resulting in passive confinement pressure. As the axial load increased, the cracks became more prominent and wider, occasionally resulting in mortar separation and bulging, as shown in Figure 7. Several WWMs in the crushed specimens exhibited fractured horizontal wires, indicating that these wires yielded as a result of hoop tension.

3.5. Effect of fiber types

Figure 10 shows the compressive strength of unheated and heated specimens to evaluate the fiber

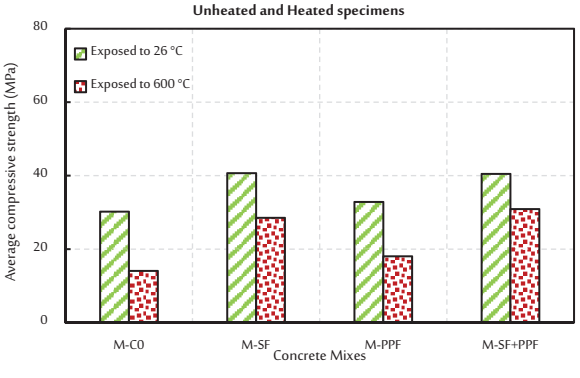

Fig. 10. Effect of fiber types on compressive strength of unheated and heated specimens

type effects on the compressive strength following exposure to high temperatures. This describes the residual strength of the concrete after being subjected to high temperature (i.e., 600°C) compared to its strength at room temperature (i.e., 26°C). The results presented clearly demonstrate that the inclusion of fibers has a substantial effect on the compressive strength of concrete, regardless of fiber type. Incorporating fibers significantly mitigated the decline in compressive strength caused by exposure to high temperatures compared to concrete mixes without fiber. Therefore, the decrease in the compressive strength of heated

fiber-reinforced concrete cylinders was smaller compared to the control concrete specimens (i.e., plain mix). The SF-RT, PPF-RT, and SF+PPF-RT showed an increased ratio of 34.7%, 8.9%, and 34.1%, respectively, compared to control concrete specimens (i.e., C0-RT). However, the reduction in the compressive strength of heated specimens of C0-600, SF-600, PPF-600, and SF+PPF-600 was 53.3%, 29.9%, 45.3%, and 23.7% compared to unheated specimens of C0-RT, SF-RT, PPF-RT, and SF+PPF-RT, respectively. Based on the findings provided in Figure 10, it can be generally concluded that the fibers can be ranked in terms of increasing efficiency as follows: SF alone, hybrid fibers (SF+PPF), and finally PPF alone. The steel fibers are superior because of their bridging effect. The rationale for this is that SFs have better mechanical properties (e.g., elastic modulus and strength) than PP fibers, and SFs can also endure greater temperatures. The enhanced compressive strength of the fiber-reinforced mixes can be attributed to the strong bonding effect between the concrete matrix and the fibers. This bonding effect reduces the formation and propagation of cracks, allowing the specimens to continue resisting axial loads even in the presence of cracks [53]. In addition to being shorter, PP fibers have a lower elasticity modulus and tensile strength compared to SFs. Thus, PP fibers have the ability to bridge microcracks but do not have a substantial influence on the compressive strength, which is comparable to the outcome mentioned in previous studies (e.g., [7, 56, 57]).

3.6. Influence of strengthening on the initial stiffness

The RC members' stiffness significantly influences the RC structures' load distribution. Therefore, the strengthening method for damaged RC members needs to be able to restore both stiffness and compressive strength. Enhanced understanding of the effects of being subjected to high temperatures and the WWM jacketing on the elastic behavior of the specimens was achieved by evaluating the initial stiffness of the tested cylinders. The initial stiffness was determined as a ratio of the stress to the strain at 40% of the ultimate axial load. At this stage, no cracks were detected in the cylinder specimens. Table 5 illustrates the compressive strength and initial stiffness test results for each concrete cylinder. Table 5 and Figure 9 demonstrate that subjecting the cylinder specimens to a temperature of 600°C for a duration of 3 hours resulted in a notable reduction in the initial stiffness. Regarding the exposure to a temperature of 600°C, the use of WWM jacketing as well as the presence of fibers resulted in decreased initial stiffness. The reduction in the initial stiffness of heated specimens of C0-600, SF-600, PPF-600, and SF+PPF-600 showed an increased ratio of 89.2%, 82.9%, 85.0%, and 83.7% compared to unheated specimens of C0-RT, SF-RT, PPF-RT, and SF+PPF-RT, respectively. It can be noticed that the heated specimens that had PP fiber showed the lowest initial stiffness compared to all specimens, which can be attributed to the fact that PP melts when exposed to high temperatures. However, strengthening the heated specimens led to a reduction in the loss of initial stiffness compared to the heated specimens before strengthening. For example, the initial stiffness loss reached 27.6% in the presence of SF, compared to 82.9% for the same specimen before strengthening. Nevertheless, the presence of fibers in mixes resulted in increased initial stiffness at room temperature. The SF-RT, PPF-RT, and SF+PPF-RT showed an increased ratio of 32.6%, 18.8%, and 34.1%, respectively, compared to control concrete specimens (i.e., C0-RT). In addition, the same trend was noticed when using WWM jacketing to strengthen the specimens. The C0-RT-S, SF-RT-S, PPF-RT-S, and SF+PPF-RT-S showed an increased ratio of 28.9%, 77.4%, 8.0%, and 71.8%, respectively, compared to control concrete specimens (i.e., C0-RT). The stiffness of the specimens in the elastic zone was dependent on the confinement strength and the elastic modulus of the WWM. The result showed that the PP fibers make a small contribution to the specimen's initial stiffness, which can be attributed to the PP fibers having a lower elastic modulus and tensile strength compared to SFs. The decreased initial stiffness of heated specimens is primarily attributed to the occurrence of micro-cracks caused by heat and

Table 5. Summary of test results

Specimen ID	Compressive strength		Initial stiffness	
	(MPa)	Relative Variation*	(N/mm)	Relative Variation*
C0-RT	30.2	–	20133.3	–
C0-600	14.1	-53.3%	2169.2	-89.2%
C0-RT-S	50.6	+67.5%	25948.7	28.9%
C0-600-S	29.9	−1.0%	8542.9	−57.6%
SF-RT	40.7	–	26688.5	–
SF-600	28.5	−29.9%	4560.0	−82.9%
SF-RT-S	71.0	+74.4%	47333.3	77.4%
SF-600-S	56.5	+38.8%	19316.2	−27.6%
PPF-RT	32.9	–	43866.7	–
PPF-600	18.0	−45.3%	3600.0	−85.0%
PPF-RT-S	60.1	+82.7%	25849.5	8.0%
PPF-600-S	34.5	+4.9%	11311.5	−52.7%
SF+PPF-RT	40.5	–	27000.0	–
SF+PPF-600	30.9	−23.7%	4414.3	−83.7%
SF+PPF-RT-S	66.1	+63.2%	46386.0	71.8%
SF+PPF-600-S	44.3	+9.4%	14644.6	−45.8%

* Compared to the control specimen in each mix and the positive sign indicates an increase, whereas the negative sign indicates a decrease.

the subsequent loss of water, which leads to the softening and creation of pores in the concrete. Consequently, heated concrete specimens are anticipated to display greater lateral expansion when compressed axially compared to unheated concrete specimens [13].

4. Conclusion

The main conclusions of the current study are the following:

1. After exposure to 600°C, both plain and fiber-reinforced concrete specimens lost between 23.7% and 53.3% of their compressive strengths.
2. Fibers significantly enhance concrete's compressive strength, reaching 34.7%, and mitigate the high temperature-induced decline, regardless of fiber type, compared to plain concrete specimens.
3. The WWM jacketing led to a significant increase in the specimens' compressive strengths, ranging from 63.2% to 82.7% when exposed to a temperature of 26°C. In addition, the increase ratio for exposure to a temperature of 600°C ranged from 43.4% to 112.1%.
4. Thermal cracking was observed in concrete specimens without fibers at 600°C, but fibers prevented surface cracks. Strengthened specimens exposed to 600°C showed reduced brittle failure susceptibility.
5. The results indicate that the concrete with SF exhibited a superior capacity for energy absorption (the area under the stress-strain curve) and elastic modulus following exposure to high temperatures in comparison to the concretes with no fibers, PP, and hybrid fibers.
6. The suggested approaches to strengthening, which involve the use of WWM jacketing with two layers, successfully restored and surpassed the initial concrete compressive strength of the specimens that were damaged due to exposure to high temperatures.

Declaration of Competing Interest

No conflict of interest

Acknowledgments

The authors extend their appreciation to Researchers Supporting Project number (RSP2024R343), King Saud University, Riyadh, Saudi Arabia.

References

[1] Sarker P, Kelly S, Yao Z. Effect of fire exposure on cracking, spalling and residual strength of fly ash geopolymer concrete. *Mater Des*. 2014;29: 584–592. doi: 10.1016/j.matdes.2014.06.059

[2] Shaikh FUA, Vimonsatit V. Effect of cooling methods on residual compressive strength and cracking behavior of fly ash concretes exposed at elevated temperatures. *Fire Mater*. 2016;40: 335–350. doi: 10.1002/FAM.2276

[3] Abadel A, Elsanadedy H, Almusallam T, Alaskar A, Abbas H, Al-Salloum Y. Residual compressive strength of plain and fiber reinforced concrete after exposure to different heating and cooling regimes. *Eur J Environ Civ Eng*. 2021;26: 6746–6765. doi: 10.1080/19648189.2021.1960898

[4] Li Q, Yuan G, Shu Q. Effects of heating/cooling on recovery of strength and carbonation resistance of fire-damaged concrete. *Mag Concr Res*. 2015;66: 925–936. doi: 10.1680/MACR.14.00029

[5] Kee S, Kang J, Choi B, Kwon J, Candelaria M. Evaluation of static and dynamic residual mechanical properties of heat-damaged concrete for nuclear reactor auxiliary buildings in korea using elastic wave velocity measurements. *Materials (Basel)*. 2019;12: 2695. doi: 10.3390/ma12172695

[6] Ma C, Garcia R, Yung S, Awang A, Omar W, Pilakoutas K. Strengthening of pre-damaged concrete cylinders using post-tensioned steel straps. *Proc Inst Civ Eng – Struct Build.* 2019;172(10): 703–711. doi: 10.1680/jstbu.18.00031

[7] Abadel AA, Alharbi YR. Confinement effectiveness of CFRP strengthened ultra-high performance concrete cylinders exposed to elevated temperatures. *Mater Sci*. 2021;39: 478–490. doi: 10.2478/MSP-2021-0040

[8] Zhai C, Chen L, Fang Q, Chen W, Jiang X. Experimental study of strain rate effects on normal weight concrete after exposure to elevated temperature. *Mater Struct*. 2017;50: 40.

[9] Martins DJ, Correia JR, de Brito J. The effect of high temperature on the residual mechanical performance of concrete made with recycled ceramic coarse aggregates. *Fire Mater*. 2016;40: 289–304.

[10] Abadel AA. Rehabilitation of post-heated rectangular reinforced concrete columns using different strengthening configuration. *Struct. Concr*. 2023. doi: 10.1002/SUCO.202300521

[11] Khan MS, Abbas H. Performance of concrete subjected to elevated temperature. *Eur J Env. Civ En*. 2016;20: 532–543.

[12] Abadel AA, Khan MI, Masmoudi R. Axial capacity and stiffness of post-heated circular and square columns strengthened with carbon fiber reinforced polymer jackets. *Structures*. 2021;33: 2599–2610. doi: 10.1016/j.istruc.2021.05.081

[13] Abadel AA, Masmoudi R, Iqbal Khan M. Axial behavior of square and circular concrete columns confined with CFRP sheets under elevated temperatures: Comparison with welded-wire mesh steel confinement. *Structures*. 2022;45: 126–144. doi: 10.1016/J.ISTRUC.2022.09.026

[14] Drzymała T, Jackiewicz-Rek W, Tomaszewski M, Kuś A, Gałaj J, Šukys R. Effects of high temperature on the properties of high performance concrete (HPC). *Procedia Eng*. 2017;172: 256–263.

[15] Elsanadedy HM. Residual compressive strength of high-strength concrete exposed to elevated temperatures. *Adv Mater Sci Eng*. 2019.

[16] Abbas H, Al-Salloum YA, Elsanadedy HM, Ann ATH. Models for prediction of residual strength of HSC after exposure to elevated temperature. *Fire Saf J*. 2019;106: 13–28.

[17] Al-Salloum YA, Elsanadedy HM, Abadel AA. Behavior of FRP-confined concrete after high temperature exposure. *Constr Build*. 2011;25: 838–850. doi: 10.1016/j.conbuildmat.2010.06.103

[18] Phan LT, Lawson JR, Davis FL. Effects of elevated temperature exposure on heating characteristics, spalling, and residual properties of high performance concrete. *Mater Struct*. 2001 342. 2001;34: 83–91. doi: 10.1007/BF02481556

[19] Vkr K, Wang TC, Cheng FP. Predicting the fire resistance behaviour of high strength concrete columns. *Cem Concr Comp* 2004;26: 141–153.

[20] Aslani F, Bastami M. Constitutive relationships for normal-and high-strength concrete at elevated temperatures. *ACI Mater J*. 2011;108: 355–364. doi: 10.14359/51683106

[21] Abadel A, Abbas H, Albidah A, Almusallam T, Al-Salloum Y. Effectiveness of GFRP strengthening of normal and high strength fiber reinforced concrete after exposure to heating and cooling. *Eng Sci Technol an Int J*. 2022;36: 101147. doi: 10.1016/J.JESTCH.2022.101147

[22] Gong W, Ueda T. Basic study on chloride-induced steel corrosion in concrete subjected to heating up to 300°C. *J Soc Mater Sci Japan*. 2018;67: 738–745. doi: 10.2472/jsms.67.738

[23] Choe G, Kim G, Gucunski N, Lee S. Evaluation of the mechanical properties of 200 MPa ultra-high-strength concrete at elevated temperatures and residual strength of column. *Constr Build Mater*. 2015;86: 159–168.

[24] Lee C, Kee S, Kang J, Choi B, Lee J. Interpretation of impact-echo testing data from a fire-damaged reinforced concrete slab using a discrete layered concrete damage model. *Sensors*. 2020;20: 5838. doi: 10.3390/s20205838

[25] Vu G, Timothy J, Saenger E, Meschke G. Damage identification in concrete using multiscale computational modeling and convolutional neural networks. *Pamm*. 2021;21. doi: 10.1002/pamm.202100249

[26] Li Z, Xu J, Bai E. Static and dynamic mechanical properties of concrete after high temperature exposure. *Mater Sci Eng*. 2012;544: 27–32.

[27] Chen L, Fang Q, Jiang X, Ruan Z, Hong J. Combined effects of high temperature and high strain rate on normal weight concrete. *Int J Impact Eng*. 2016;2015: 25–37.

[28] Xiao J, Li Z, Xie Q, Shen L. Effect of strain rate on compressive behaviour of high-strength concrete after exposure to elevated temperatures. *Fire Saf J*. 2016;83: 25–37. doi: 10.1016/J.FIRESAF.2016.04.006

[29] Poon CS, Azhar S, Anson M, Wong YL. Comparison of the strength and durability performance of normal- and high-strength pozzolanic concretes at elevated temperatures. *Cem Concr Res*. 2001;31: 1291–1300. doi: 10.1016/S0008-8846(01)00580-4

[30] Bastami M, Chaboki-Khiabani A, Baghbadrani M, Kordi M. Performance of high strength concretes at elevated temperatures. *Sci Iran*. 2011;18: 1028–1036. doi: 10.1016/j.scient.2011.09.001

[31] Ning X, Li J, Li Y. An explorative study into the influence of different fibers on the spalling resistance and mechanical properties of self-compacting concrete after exposure to elevated temperatures. *Appl Sci*. 2022;12: 12779. doi: 10.3390/APP122412779

[32] Freitas Resende H, Nascimento Arroyo F, Dias Reis E, Chahud E, Ferreira dos Santos H, Tostes Linhares JA, Garcez de Azevedo AR, Christoforo AL, Melgaço Nunes Branco LA. Estimation of physical and mechanical properties of high-strength concrete with polypropylene fibers in high-temperature condition. *J Mater Res Technol*. 2023;24: 8184–8197. doi: 10.1016/J.JMRT.2023.05.085

[33] Bayasi Z, Al Dhaheri M. Effect of exposure to elevated temperature on polypropylene fiber-reinforced concrete. *Mater J*. 2002;99: 22–26.

[34] Bangi MR, Horiguchi T. Effect of fibre type and geometry on maximum pore pressures in fibre-reinforced high strength concrete at elevated temperatures. *Cem Concr Res*. 2012;42: 459–466. doi: 10.1016/J.CEMCONRES.2011.11.014

[35] Novák J, Kohoutková A. Fire response of Hybrid Fiber Reinforced Concrete to High Temperature. *Procedia Eng*. 2017;172: 784–790. doi: 10.1016/j.proeng.2017.02.123

[36] Varona FB, Baeza FJ, Bru D, Ivorra S. Influence of high temperature on the mechanical properties of hybrid fibre reinforced normal and high strength concrete. *Constr Build Mater*. 2018;159: 73–82. doi: 10.1016/J.CONBUILDMAT.2017.10.129

[37] Siddika A, Shojib M, Hossain M, Mamun M, Alyousef R, Amran M. Flexural performance of wire mesh and geotextile-strengthened reinforced concrete beam. *Sn Appl Sci*. 2019;1. doi: 10.1007/s42452-019-1373-8

[38] Dębska A, Gwoździewicz P, Seruga A, Balandraud X, Destrebecq J. The application of ni–ti sma wires in the external prestressing of concrete hollow cylinders. *Materials (Basel)*. 2021;14: 1354. doi: 10.3390/ma14061354

[39] El-sayed TA. Axial compression behavior of ferrocement geopolymer HSC Columns. *Polym*. 2021;13: 3789. doi: 10.3390/POLYM13213789

[40] Mourad SM, Shannag MJ. Repair and strengthening of reinforced concrete square columns using ferrocement jackets. *Cem*. 2012;34: 288–294. doi: 10.1016/j.cemconcomp.2011.09.010

[41] Elsibaey M, Awadallah Z, Zakaria M, Farghal O. Strengthening of reinforced concrete square columns by means of ferro cement jacket. *Jes J Eng Sci*. 2020;48(5): 888–909. doi: 10.21608/jesaun.2020.118571

[42] Eltaly BA, Shaheen YB, EL-boridy AT, Fayed S. Ferrocement composite columns incorporating hollow core filled with lightweight concrete. *Eng Struct*. 2023;280: 115672. doi: 10.1016/j.engstruct.2023.115672

[43] Alobaidy QNA, Abdulla AI, Al-Mashaykhi M. Shear behavior of hollow ferrocement beam reinforced by steel and fiberglass meshes. *Tikrit J Eng Sci*. 2022;29: 27–39. doi: 10.25130/tjes.29.4.4

[44] Mabrouk R, Awad M, Abdelkader N, Kassem M. Strengthening of reinforced concrete short columns using ferrocement under axial loading. *J Eng Res*. 2022;6(3): 32-48. doi: 10.21608/erjeng.2022.154329.1083

[45] Hadi MN, Algburi AHM, Sheikh MN, Carrigan AT. Axial and flexural behaviour of circular reinforced concrete columns strengthened with reactive powder concrete jacket and fibre reinforced polymer wrapping. *Constr Build Mater*. 2018;172: 717–727. doi: 10.1016/j.conbuildmat.2018.03.196

[46] Kaish ABMA, Jamil M, Raman SN, Zain MFM, Nahar L. Ferrocement composites for strengthening of concrete columns: A review. *Constr Build Mater*. 2018;160: 326–340. doi: 10.1016/J.CONBUILDMAT.2017.11.054

[47] Kondraivendhan B, Pradhan B. Effect of ferrocement confinement on behavior of concrete. *Constr Build*. 2009;23: 1218–1222.

[48] Harmathy TZ, Berndt JE. Hydrated Portland cement and lightweight concrete at elevated temperatures. *Am Concr Inst*. 1966;63: 93–112.

[49] ISO. *Fire-resistance tests – elements of building construction – part 1: General requirements*. 1999. https://www.iso.org/standard/2576.html (accessed December 25, 2021).

[50] ASTM-C39. *Standard Test Method for Compressive Strength of Cylindrical Concrete*. West Conshohocken, PA: ASTM International, 2021. https://www.astm.org/c0039_c0039m-21.html%0Ahttps://www.astm.org/Standards/C39

[51] Al-Salloum YA, Almusallam TH, Elsanadedy HM, Iqbal RA. Effect of elevated temperature environments on the residual axial capacity of RC columns strengthened with different techniques. *Constr Build Mater*. 2016;115: 345–361. doi: 10.1016/J.CONBUILDMAT.2016.04.041

[52] Elsanadedy H, Almusallam T, Al-Salloum Y, Iqbal R. Effect of high temperature on structural response of reinforced concrete circular columns strengthened with fiber reinforced polymer composites. *J Compos Mater*. 2017;51: 333–355. doi: 10.1177/0021998316645171/ASSET/IMAGES/LARGE/10.1177_0021998316645171-FIG20.JPEG

[53] Alshaikh, I. M., Abu Bakar, B. H., Alwesabi, E. A., Abadel, A. A., Alghamdi, H., & Wasim, M. . An Experimental Study on Enhancing Progressive Collapse Resistance Using Steel Fiber-Reinforced Concrete Frame . Journal of Structural Engineering. 2022;148(7): 04022087.

[54] Alwesabi EA, Abu Bakar BH, Alshaikh IMH, Akil HM. Impact resistance of plain and rubberized concrete containing steel and polypropylene hybrid fiber. *Mater Today Commun*. 2020;25: 101640. doi: 10.1016/J.MTCOMM.2020.101640

[55] Xiao J, Falkner H. On residual strength of high-performance concrete with and without polypropylene fibres at elevated temperatures. *Fire Saf J*. 2006;41: 115–121. doi: 10.1016/J.FIRESAF.2005.11.004

[56] Alwesabi EAH, Bakar BHA, Alshaikh IMH, Akil HM. Experimental investigation on mechanical properties of plain and rubberised concretes with steel–polypropylene hybrid fibre. *Constr Build Mater*. 2020;233: 117194. doi: 10.1016/J.CONBUILDMAT.2019.117194

[57] Abadel A, Abbas H, Almusallam T, Al-Salloum Y, Siddiqui N. Mechanical properties of hybrid fibre-reinforced concrete – analytical modelling and experimental behaviour. *Mag Concr Res*. 2016;68: 823–843. doi: 10.1680/JMACR.15.00276

Received 2024-05-13
Accepted 2024-06-30